Colloquia: LaThuile11

Electroweak and Top physics at ATLAS

A. R. Sandström on behalf of the ATLAS Collaboration

Max-Planck-Institut für Physik, (Werner-Heisenberg-Institut) - Föhringer Ring 6,
80805 München, Germany
Nikhef National Institute for Subatomic Physics, and University of Amsterdam
Science Park 105, 1098 XG Amsterdam, The Netherlands

Summary. — The observations of electroweak boson (W, Z) and top quark pair $(t\bar{t})$ production are among the key milestones for the early LHC physics programme. Production of $t\bar{t}$, W and Z in association with jets are important backgrounds in various searches for physics beyond the Standard Model, and new physics may also give rise to additional production mechanisms or modification of the decay channels. This note summarizes the electroweak and top physics performed in ATLAS with $\sqrt{s} = 7$ TeV proton-proton collisions during 2010 and compares the observations with theoretical predictions.

PACS 14.65.Ha – Top quarks.
PACS 14.70.Fm – W bosons.
PACS 14.70.Hp – Z bosons.

1. – Introduction

The ATLAS experiment [1] at the Large Hadron Collider recorded more than $40\,\mathrm{pb}^{-1}$ at $\sqrt{s} = 7$ TeV proton-proton collisions during 2010. This note summarizes some of the tests of the Standard Model that were performed with integrated luminosity ranging from 0.3 to $31\,\mathrm{pb}^{-1}$. The note first covers the results using electroweak bosons before presenting results using top quarks.

2. – Electroweak results

2˙1. *W/Z cross section*. – At hadron colliders, the W and Z bosons can most easily be detected via their leptonic decay mode. The ATLAS experiment observed $W \to e\nu$, $W \to \mu\nu$, $Z \to ee$, and $Z \to \mu\mu$ candidates produced from the $\sqrt{s} = 7$ TeV proton-proton collisions of the LHC [2]. The measurements are based on data corresponding to an integrated luminosity of approximately $0.3\,\mathrm{pb}^{-1}$. The absolute luminosity was calibrated using beam separation scans, yielding a total systematic uncertainty of $\pm 11\%$ [3], dominated by the measurement of the LHC beam currents.
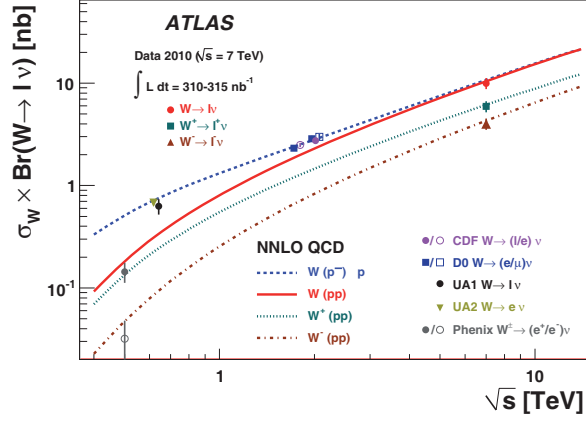
Fig. 1. – The measured values of $\sigma_W \times \mathrm{BR}(W \to l\nu)$ for W^+, W^- and for their sum compared to the theoretical predictions based on NNLO QCD calculations. Results are shown for the combined electron-muon results. The predictions are shown for both proton-proton (W^+, W^- and their sum) and proton-antiproton colliders (W) as a function of $\sqrt{s}$. In addition, previous measurements at proton-antiproton and proton-proton colliders are shown. The data points at the various energies are staggered to improve readability. The CDF and D0 measurements are shown for both Tevatron collider energies, $\sqrt{s} = 1.8\,\mathrm{TeV}$ and $\sqrt{s} = 1.96\,\mathrm{TeV}$. All data points are displayed with their total uncertainty. The theoretical uncertainties are not shown [2].

Muons are required to have at least one combined muon track with $p_\mathrm{T} > 20\,\mathrm{GeV}$ and p_T measured by the muon spectrometer (MS) alone greater than $p_\mathrm{T}^\mathrm{MS} > 10\,\mathrm{GeV}$, within the range $|\eta_\mu| < 2.4$. Electron tracks are required to have $E_\mathrm{T} > 20\,\mathrm{GeV}$ and $|\eta| < 2.47$ where candidates in the calorimeter transition region $1.37 < |\eta| < 1.52$ are excluded. $Z \to ll$ candidates are required to have two leptons of the same flavour and opposite charge. W candidates are selected by requiring one lepton and missing transverse energy $E_\mathrm{T}^\mathrm{miss} > 25\,\mathrm{GeV}$. Furthermore, a transverse mass requirement $m_\mathrm{T} > 40\,\mathrm{GeV}$ is imposed on W candidates, where

$$(1) \qquad m_\mathrm{T} = \sqrt{2 p_\mathrm{T}^l p_\mathrm{T}^\nu (1 - \cos(\phi^l - \phi^\nu))}\,,$$

and where the highest p_T lepton is used and the (x, y) components of the neutrino momentum are inferred from the corresponding $E_\mathrm{T}^\mathrm{miss}$ components.

The $W \to l\nu$ analysis resulted in a total of 1069 candidates pass all requirements in the electron channel and 1181 candidates in the muon channel. The $Z \to ll$ found a total of 70 candidates pass all requirements in the electron channel and 109 candidates in the muon channel, within the invariant mass window $66 < m_{ll} < 116\,\mathrm{GeV}$. After correcting for acceptance and inefficiencies these observations lead to the measured cross sections

$$(2) \qquad \sigma_W \times \mathrm{BR}(W \to l\nu) = 9.96 \pm 0.23(\mathrm{stat}) \pm 0.50(\mathrm{syst}) \pm 1.10(\mathrm{lumi})\ \mathrm{nb},$$

$$(3) \qquad \sigma_{Z/\gamma^\star} \times \mathrm{BR}(Z/\gamma^\star \to ll) = 0.82 \pm 0.06(\mathrm{stat}) \pm 0.05(\mathrm{syst}) \pm 0.09(\mathrm{lumi})\ \mathrm{nb}.$$

These results are shown in figs. 1 and 2, together with results at lower center-of-mass energies. Theoretical predictions, based on NNLO QCD calculations, are in good agreement with these measurements.
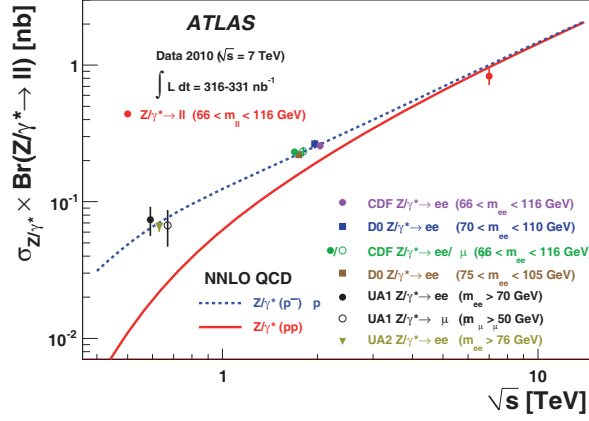
Fig. 2. – The measured value of $\sigma_Z/\gamma^\star \times \mathrm{BR}(Z/\gamma^\star \to ll)$ where the electron and muon channels have been combined, compared to the theoretical predictions based on NNLO QCD calculations. The predictions are shown for both proton-proton and proton-antiproton colliders as a function of $\sqrt{s}$. In addition, previous measurements at proton-antiproton and proton-proton colliders are shown. The data points at the various energies are staggered to improve readability. The CDF and D0 measurements are shown for both Tevatron collider energies, $\sqrt{s} = 1.8$ TeV and $\sqrt{s} = 1.96$ TeV. All data points are displayed with their total uncertainty. The theoretical uncertainties are not shown [2].

The measurement of the ratio of the W to Z cross sections times branching ratios constitutes an important test of the Standard Model. It can be measured with a higher relative precision than the individual cross sections since both experimental and theoretical uncertainties partially cancel. The observed ratio is

$$(4) \qquad\qquad R_{W/Z} = 11.7 \pm 0.9(\text{stat}) \pm 0.4(\text{syst}),$$

whereas the theoretical prediction is $R_{W/Z} = 10.840 \pm 0.054$ [4, 5].

2˙2. *W charge asymmetry*. – The measurement of the charge asymmetry of leptons originating from the decay of singly produced W bosons at pp, $p\bar{p}$ and ep colliders provides important information about the proton structure as described by parton distribution functions (PDFs). The W boson charge asymmetry is mainly sensitive to valence quark distributions via the dominant production process $u\bar{d}(\bar{u}d) \to W^{+(-)}$ and provides complementary information to that obtained from measurements of inclusive deep inelastic scattering cross sections at the HERA electron-proton collider [6].

The ATLAS experiment has measured the muon charge asymmetry from the decay of $W^{\pm}$ bosons in pp collisions at a centre-of-mass energy of $\sqrt{s} = 7$ TeV at the LHC [7]. The asymmetry varies significantly as a function of the pseudorapidity. The muon charge asymmetry A_μ is defined from the cross sections for $W \to \mu\nu$ production $\mathrm{d}\sigma_{\mathrm{W}\mu^\pm}/\mathrm{d}\eta_\mu$ as

$$(5) \qquad\qquad A_\mu = \frac{\mathrm{d}\sigma_{\mathrm{W}\mu^+}/\mathrm{d}\eta_\mu - \mathrm{d}\sigma_{\mathrm{W}\mu^-}/\mathrm{d}\eta_\mu}{\mathrm{d}\sigma_{\mathrm{W}\mu^+}/\mathrm{d}\eta_\mu + \mathrm{d}\sigma_{\mathrm{W}\mu^-}/\mathrm{d}\eta_\mu},$$

where the cross sections include the event kinematical cuts used to select $W \to \mu\nu$

events. Systematic effects on the W-production cross section measurements are typically the same for positive and negative muons, mostly canceling in the asymmetry. The results presented are based on data collected in 2010 with an integrated luminosity of $31\,\text{pb}^{-1}$. The W candidate events were selected with the same kinematical cuts as in the $W \to l\nu$ analysis described above.

The W yield is corrected for reconstruction inefficiencies by correction factors corresponding to the ratio of reconstructed over generated events in the simulated W sample, satisfying all kinematic requirements of the event selection. No extrapolation to the full phase space is attempted in order to reduce the dependence on theoretical predictions.

The main backgrounds to $W \to \mu\nu$ arise from heavy flavour decays in multijet events and from the electro-weak background from $W \to \tau\nu$ with a semi-muonic tau decay, $Z \to \mu\mu$ where one muon is not reconstructed and produces fake $E_{\mathrm{T}}^{\text{miss}}$, and $Z \to \tau\tau$ with a semi-muonic tau decay, as well as semileptonic $t\bar{t}$ decays in the muon channel. The $W \to \tau\nu$ contribution is treated as a background.

The dominant sources of systematic uncertainty on the asymmetry come from the trigger and reconstruction efficiencies. There is a loss of trigger efficiency in the low pseudorapidity region due to reduced geometric acceptance, resulting in a larger statistical error. As a result, the trigger systematic uncertainty on the asymmetry is largest in the low pseudorapidity bins (6–7% for central $|\eta_\mu|$ and 2–3% for forward $|\eta_\mu|$). Similarly, the uncertainty associated with the reconstruction efficiency is in average 1–2% but can be up to 7% in certain detector regions. The systematic uncertainties due to the QCD background is 1–2% and arise primarily from the uncertainty on the isolation efficiency for muons in QCD events. The combination the other backgrounds results in an uncertainty on the asymmetry of less than 1%. The impact of using an NLO MC using the CTEQ 6.6 [8] PDF rather than PYTHIA with MRST LO PDF [5] in the correction factor calculation has been evaluated and an additional systematic uncertainty of about 3% is included to account for the theoretical modelling.

The measured differential muon charge asymmetry in eleven bins of muon absolute pseudorapidity is shown in fig. 3. The statistical and systematic uncertainties per $|\eta_\mu|$ bin are included and contribute comparably to the total uncertainty. Figure 3 also show expectations for the muon asymmetry from W predictions at NLO with different PDF sets: CTEQ 6.6, HERA 1.0 [6] and MSTW 2008 [9]; all predictions are presented with 90% confidence level error bands. While the predictions with different PDF sets differ within their respective uncertainty bands, they follow the same global trend. The measured asymmetry agrees with this expectation. As demonstrated graphically in fig. 3, all PDF sets are compatible with the data.

3. – Top cross section

In the Standard Model (SM) the $t\bar{t}$ production cross section in pp collisions is calculated to be $164.6 \, ^{+11.4}_{-15.7} \, \text{pb}$ [10] at a centre of mass energy $\sqrt{s} = 7\,\text{TeV}$ assuming a top mass of $172.5\,\text{GeV}$, and top quarks are predicted to decay to a W boson and a b-quark ($t \to Wb$) nearly 100% of the time. Events with a $t\bar{t}$ pair can be classified as "single-lepton", "dilepton", or "all hadronic" by the decays of the two W bosons: a pair of quarks ($W \to q\bar{q}$) or a lepton-neutrino pair ($W \to \ell\nu$), where ℓ refers to a lepton. The production of $t\bar{t}$ at the LHC is dominated by gg fusion.

The results described in this note are based on reconstructed electrons and muons and include small contributions from leptonically decaying tau leptons. The single-lepton
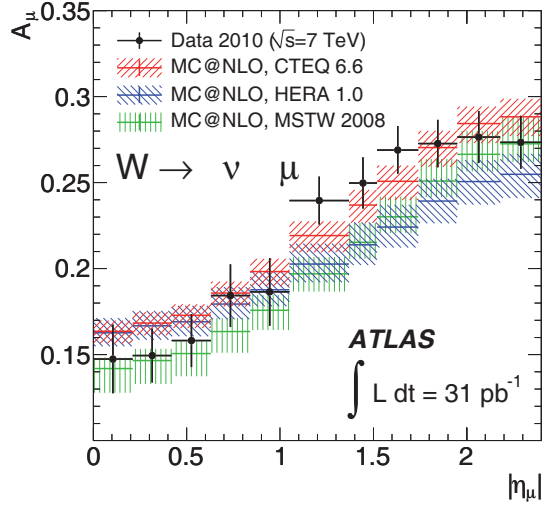
Fig. 3. – The muon charge asymmetry from W-boson decays in bins of absolute pseudorapidity. The kinematic requirements applied are muon $p_T > 20\,\text{GeV}$, neutrino $p_T > 25\,\text{GeV}$ and $m_T > 40\,\text{GeV}$. The data points (shown with error bars including the statistical and systematic uncertainties) are compared to MC@NLO predictions with different PDF sets. The PDF uncertainty bands are described in the text and include experimental uncertainties as well as model and parametrization uncertainties [7].

mode, with a branching ratio([1]) of 37.9% (combining e and μ channels), and the dilepton mode, with a branching ratio of 6.5% (combining ee, $\mu\mu$ and $e\mu$ channels), both give rise to final states with at least one lepton, missing transverse energy and jets, some with b flavour. The cross section measurements in both modes are based on a straightforward counting method using $2.9\,\text{pb}^{-1}$ of integrated luminosity. The number of signal events is obtained in a signal enriched sample after background subtraction. The main background contributions are determined using data-driven methods, since the theoretical uncertainties on the normalisation of these backgrounds are relatively large.

3.1. *Single-lepton channel.* – The single lepton $t\bar{t}$ final state is characterized by an isolated lepton with relatively high p_T and missing transverse energy corresponding to the neutrino from the W leptonic decay, two b quark jets and two light jets from the hadronic W decay. Events with at least four jets with $p_T > 25\,\text{GeV}$, where at least one of the jets with is tagged as a b-jet, and exactly one reconstructed lepton (electron or muon) with $p_T > 20\,\text{GeV}$ and $E_T^{\text{miss}} > 20\,\text{GeV}$ and $E_T^{\text{miss}} + m_T(W) > 60\,\text{GeV}$ where considered as $t\bar{t}$ signal candidates. Muon tracks and jets are reconstructed within the geometrical acceptance of the inner detector, $|\eta| < 2.5$. Electrons are selected using the same pseudorapidity regions as used in the W/Z cross section measurements.

For the QCD multi-jet and W + jets backgrounds, data-driven estimates are used, while for the expected background from Z+jets and single-top production, simulation

---

([1]) The quoted branching ratios also include small contributions from leptonically decaying tau leptons.

estimates are used. The W + jet background is estimated from the measurement of fraction the of $W + 2$ jets that are b-tagged. The fraction of the $W + 4$ jets events that are b-tagged is obtained by a theoretical correction factor for differences in the event flavour composition for the different jet multiplicities. This fraction together with the fact that the ratio of $W + n + 1$ jets to $W + n$ jets is approximately constant as a function of n [11] is used to estimate the background passing the b-tagged $W + 4$ jets requirement.

The QCD multi-jet background in the muon channel was estimated by using non-isolated muons. $Z \rightarrow \mu\mu$ events were used to estimate the fraction of muons from W decays that pass into the signal region from this control region. The fraction of muons from QCD multi-jet events that pass into the signal region was estimated using two regions which are enriched with muons from QCD processes. In the electron channel the QCD multi-jet background was estimated by template fitting E_T^{miss} where the template for the background was extracted from two QCD-dominated control regions.

The electron channel yields 17 events passing all cuts, while for muons 20 events are observed. Of these 37 events 12.2 ± 3.9 are estimated to be background, thereby yielding an estimated $24.8 \pm 6.1(\text{stat}) \pm 3.9(\text{syst})$ single lepton $t\bar{t}$ events.

3'2. *Dilepton channel*. – The dilepton $t\bar{t}$ final state is characterized by two isolated leptons with relatively high p_T, missing transverse energy corresponding to the neutrinos from the W leptonic decays, and two b quark jets. Events with at least two jets with $p_T > 20$ GeV, and exactly two oppositely charged leptons (electron or muon) with $p_T > 20$ GeV where considered as $t\bar{t}$ signal candidates. The pseudorapidity regions where leptons and jets are considered are the same as in the single lepton analysis described above. In addition, to suppress background from Z + jets and QCD multi-jet events in the ee channel, the missing transverse energy must satisfy $E_T^{miss} > 40$ GeV, and the invariant mass of the two leptons must differ by at least 5 GeV from the Z boson mass, *i.e.* $|m_{ee} - m_Z| > 5$ GeV. For the muon channel, the corresponding requirements are $E_T^{miss} > 30$ GeV and $|m_{\mu\mu} - m_Z| > 10$ GeV. Events in the $e\mu$-channel are required to have a the scalar sum of the transverse energies of the two leptons and all selected jets larger than 150 GeV.

A total of 9 events (2 ee, 3 $\mu\mu$ and 4 $e\mu$) passed the selection. For the ee and $\mu\mu$ channels the Z + jets is the largest background. It was estimated by a Z enriched control region scaled by the fraction of simulation events in the control region that passes into the signal region.

3'3. *Combination of subchannels*. – The combined measurement of the $t\bar{t}$ production cross-section is based on a likelihood fit in which the number of expected events is modeled as

$$(6) \qquad N^{exp}(\sigma_{t\bar{t}}, \alpha_j) = L \cdot \epsilon_{t\bar{t}}(\alpha_j) \cdot \sigma_{t\bar{t}} + \sum_{bkg} L \cdot \epsilon_{bkg}(\alpha_j) \cdot \sigma_{bkg}(\alpha_j) + N_{DD}(\alpha_j),$$

where L is the integrated luminosity, $\epsilon_{t\bar{t}}$ is the signal acceptance, ϵ_{bkg}, σ_{bkg} are the efficiency and cross section for backgrounds as obtained from MC simulation respectively, and N_{DD} is the number of expected events from data-driven estimates. The acceptance and background estimates depend on sources of systematic uncertainty labelled as α_j.

Table I lists the cross sections and signal significance for the single-lepton, dilepton and the combined channels with the corresponding statistical and systematic uncertainties extracted from the likelihood fit. By combining all five channels, the background-only hypothesis is excluded at a significance of 4.8σ obtained with the approximate method

TABLE I. – *Summary of $t\bar{t}$ cross-section and signal significance calculated by combining the single-lepton and dilepton channels individually and for all channels combined.*

	Cross section [pb]	Signal significance [σ]
Single-lepton channels	$142 \pm 34^{+50}_{-31}$	4.0
Dilepton channels	$151\ ^{+78}_{-62}\ ^{+37}_{-24}$	2.8
All channels	$145 \pm 31^{+42}_{-27}$	4.8

of [12]. These results have been cross checked with two independent fit based methods, and the results are consistent.

Figure 4 shows the ATLAS and CMS measurements together with previous Tevatron measurements. The measured $t\bar{t}$ cross-section is in good agreement with the measurement in the dilepton channel by CMS [15], as well as with approximate NNLO top quark cross section calculation [13].

4. – Summary and conclusion

The ATLAS Collaboration presents first measurements of the $W \to l\nu$ and $Z \to l\nu$ production cross sections in proton-proton collisions at $\sqrt{s} = 7\,\text{TeV}$ with an integrated luminosity of approximately $320\,\text{nb}^{-1}$. Theoretical predictions, based on NNLO QCD calculations, are in good agreement with all measurements.

The measurement of the W charge asymmetry in pp collisions at $\sqrt{s} = 7\,\text{TeV}$ performed in the $W \to \mu\nu$ decay mode using $31\,\text{pb}^{-1}$ of data is expected to contribute to
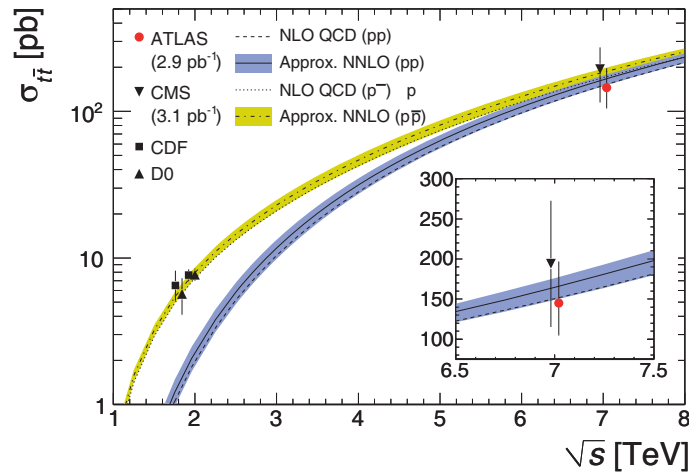

Fig. 4. – Top quark pair-production cross section at hadron colliders as measured by CDF and D0 at Tevatron, CMS and ATLAS (this measurement). The theoretical predictions for proton-proton and proton-antiproton collisions include the scale and PDF uncertainties, obtained using the HATHOR tool [13] with the CTEQ6.6 PDFs and assume a top-quark mass of 172.5 GeV [14].

the determination of the next generation of PDF sets, helping reduce PDF uncertainties, particularly the shapes of the valence quark distributions in the low-x region.

The ATLAS Collaboration measured the $t\bar{t}$ production cross section to be

$$(7) \qquad 145 \pm 31^{+42}_{-27}\,\text{pb}$$

with $2.9\,\text{pb}^{-1}$ of proton-proton data at $\sqrt{s} = 7\,\text{TeV}$ using both single lepton and dilepton decay channels. This result is in good agreement with expectations and the CMS result.

REFERENCES

[1] ATLAS Collaboration, *JINST*, **3** (2008) S08003.
[2] ATLAS Collaboration, *JHEP*, **12** (2010) 060, arXiv:1010.2130.
[3] ATLAS Collaboration, "Luminosity determination using the atlas detector," Technical Report ATLAS-CONF-2010-060, CERN, Geneva, July 2010.
[4] Anastasiou C., Dixon L., Melnikov K. and Petriello F., *Phys. Rev. D*, **69** (2004) 094008.
[5] Sherstnev A. and Thorne R. S., *Eur. Phys. J. C*, **55** (2008) 553.
[6] H1 and ZEUS Collaborations, *JHEP*, **01** (2010) 109, arXiv:0911.0884.
[7] ATLAS Collaboration (Aad *et al.*), *Phys. Lett. B*, **701** (2011) 31, arXiv:1103.2929.
[8] Pumplin J. *et al.*, *JHEP*, **07** (2002) 012, arXiv:hep-ph/0201195.
[9] Martin A. D., Stirling W. J., Thorne R. S. and Watt G., *Eur. Phys. J. C*, **63** (2009) 189.
[10] Moch S. and Uwer P., *Phys. Rev. D*, **78** (2008) 034003.
[11] Berger C., Bern Z., Dixon L. J., Cordero F., Forde D. *et al.*, *Phys. Rev. Lett.*, **106** (2011) 092001, arXiv:1009.2338.
[12] Cowan G., Cranmer K., Gross E. and Vitells O., *Eur. Phys. J. C*, **71** (2011) 1554, arXiv:1007.1727.
[13] Aliev M., Lacker H., Langenfeld U., Moch S., Uwer P. *et al.*, *Comput. Phys. Commun.*, **182** (2011) 1034, arXiv:1007.1327.
[14] ATLAS Collaboration, *Eur. Phys. J. C*, **71** (2011) 1577, arXiv:1012.1792.
[15] Khachatryan V. *et al.*, *Phys. Lett. B*, **695** (2011) 424, arXiv:1010.5994.